DOI: http://dx.doi.org/10.12989/was.2008.11.5.391

Design of aerodynamic stabilizing cables for a cable-stayed bridge during construction

Sung-Won Choi

DM engineering, Bangii-dong, Songpa-ku, Seoul, 138-050, Korea

Ho-Kyung Kim*

Department of Civil Engineering, Mokpo National University, Muan-gun, Jeonnam, 534-729, Korea
(Received June 26, 2008, Accepted July 28, 2008)

Abstract. A design procedure of stabilizing cable is proposed using buffeting analysis to stabilize the seesaw-like motion of the free cantilevered structure of a cable-stayed bridge during its construction. The bridge examined is a composite cable-stayed bridge having a main span length of 500 m. Based on the buffeting analysis, the stress in bare structure exceeded the allowable limit and a set of stabilizing cable was planned to mitigate the responses. The most efficient positions of the hold-down stabilizing cables were numerically investigated by means of an FE-based buffeting analysis and the required dimensions and pretension of the stabilizing cables were also calculated. The proposed stabilizing measure would be expected to secure the aerodynamic safety of a cantilevered structure under construction with considerable mitigation of buffeting responses.

Keywords: buffeting; stabilizing cable; cable-stayed bridge; construction; design.

1. Introduction

Recent cable-stayed bridges have made record-breaking advances in span length. Following the successful construction of the Tatara Bridge with a main span length of 890 m, the Stonecutters Bridge and Sutong Bridge are leading a new era of cable-stayed bridges that exceed 1km in main span length.

As a sea-crossing bridge, cable-stayed bridges are one of competitive alternatives for minimizing erection-related equipment or facilities such as temporary bents supporting superstructures. The balanced cantilever construction can utilize stayed cables as girder supports and enables superstructures to be erected very efficiently. It is well known, however, that this type of free cantilever construction is very vulnerable to up-coming wind turbulence.

Vibrations in long cantilevered girders are resisted mainly by pylons and, as a result, along-bridge-axis bending moment in pylons may exceed the permissible range. Obviously this phenomenon originates from a relatively less restrained structural system that behaves like a single degree-of-

* Professor, Corresponding Author, E-mail: hkkim@mokpo.ac.kr

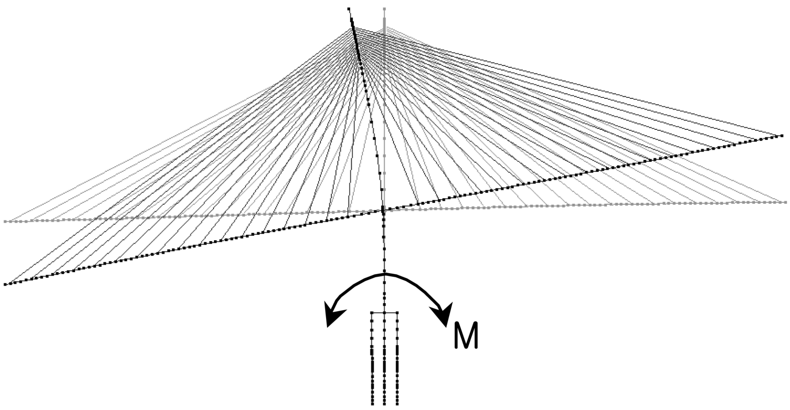

Fig. 1 Seesaw motion of free-cantilevered structure during construction

Table 1 Typhoons that influenced the Korean Peninsular

Year	Name of typhoon	Landing date
2004	MINDULLE	2004-07-04
	NAMTHEUN	2004-08-01
	MEGI	2004-08-18
	CHABA	2004-08-30
	SONGDA	2004-09-07
	HAIMA	2004-09-14
	MEARI	2004-09-29
2003	LINFA	2003-05-31
	SOUDELOR	2003-06-19
	ETAU	2003-08-08
	MAEMI	2003-09-12
2002	RAMMASUN	2002-07-06
	NAKRI	2002-07-13
	FENGSHEN	2002-07-26
	RUSA	2002-08-31
2001	PABUK	2001-08-20
2000	KAI-TAK	2000-07-10
	BOLAVEN	2000-07-30
	BILIS	2000-08-27
	PRAPIROON	2000-08-31
	SAOMAI	2000-09-15

freedom structure with rigid motion of the long-span cantilevered superstructure, as shown in Fig. 1.

Table 1 shows the list of typhoons that struck southern coast of the Korean Peninsular where a series of construction projects of sea-crossing bridges are currently underway or planned. As shown in Table 1, at least one typhoon per year struck this area and 7 were recorded in 2004. For this reason, the mitigation of buffeting responses during construction should be regarded as a key issue in on-going long-span bridge projects in Korea.

Up to present, plenty of works are accumulated with related to the buffeting analysis in the frequency domain or time domain approaches. In celebrating the historical advance in span length of the Normandy Bridge, there was a conference in Deauville, France and several papers were reported for the buffeting analysis of cable-stayed bridges during construction. Larose and Livesey (1994) and Conti, *et al*. (1994) addressed the effects of winds on the Normandy Bridge during erection phase and proposed the use of TMD for the mitigation of lateral response. Virlogeux (1992) also introduced several solutions of buffeting mitigation for the Normandy Bridge including potential stabilizing cables for the cantilevers before closure. Shum, *et al*. (2006) proposed a semi-active tuned liquid damper for the control of the lateral and torsional vibration of a cable-stayed bridge during construction. These papers, however, mainly focused on horizontal stabilization of the superstructure because of the heaving motion being controlled by the internal piers in side spans.

Kimura, *et al*. (1994) demonstrated the effect of yawed wind in buffeting analysis of the erection stage structures. Tanaka, *et al*. (1998) discussed relevant issues on the buffeting responses of long-span bridges during erection. Chauvin, *et al*. (1994) briefly introduced stabilizing tie-cable effects on the buffeting behavior of a cable-stayed bridge.

Even though stabilizing cables have been discussed in couple of papers (Virlogeux 1992, Chauvin, *et al*. 1994), a design procedure of the stabilizing cables is not fully demonstrated by utilizing the buffeting analysis, particularly for the mitigation of the vertical response for the free-cantilevered structures.

Several measures can be considered for mitigating turbulence-induced buffeting responses during construction to prevent the first-mode seesaw-like motion, as shown in Fig 2. Fig. 2(a) shows inclined temporary supports near a pylon. According to site conditions, temporary vertical piers in the side span can also be considered. Fig. 2(b) shows so-called stabilizing cables near a pylon or along a span. Fig. 2(c) shows another application for mitigating seesaw-like vibration, which utilizes a stabilizing cable from the top of the pylon to adjacent pier bents.

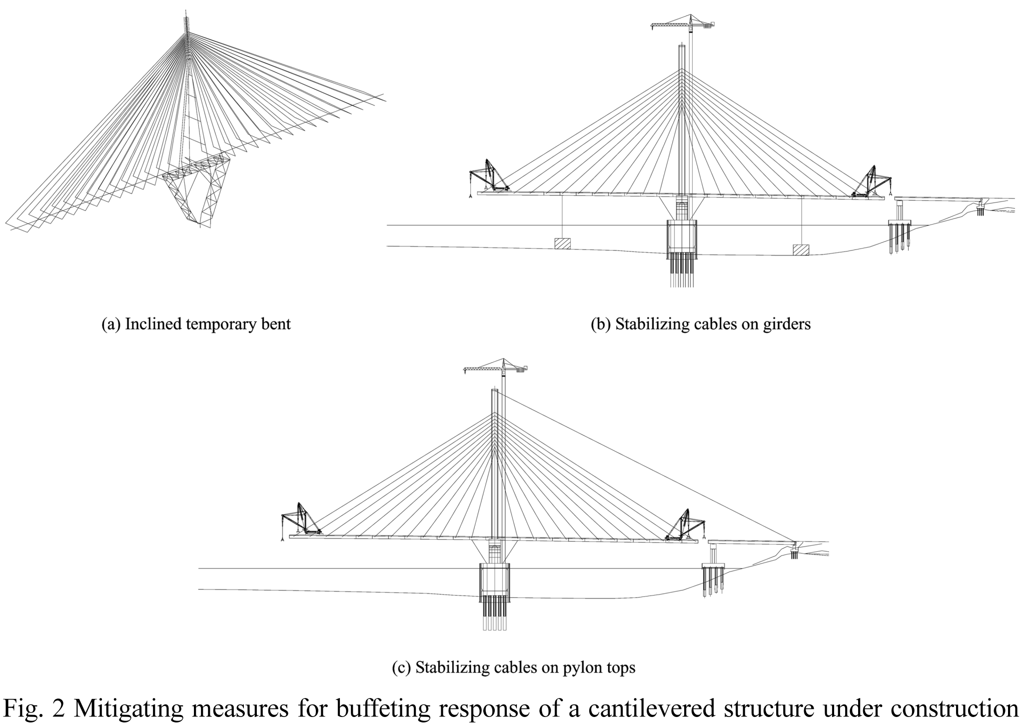

(a) Inclined temporary bent

(b) Stabilizing cables on girders

(c) Stabilizing cables on pylon tops

Fig. 2 Mitigating measures for buffeting response of a cantilevered structure under construction

Among the possible measures described above, this study chose an application involving placing stabilizing cables on both sides of cantilevered spans and a design procedure for a composite cable-stayed bridge is proposed. The design parameters include the determination of the preferred positions of stabilizing cables and the corresponding number of strands and amount of pretension. All of the design parameters were determined utilizing the FE analysis model in construction step of the structure and a frequency-domain aero-elastic buffeting analysis with flutter derivatives.

2. Generals

2.1. Examined bridge

The cable-stayed bridge investigated consists of 5 continuous spans with edge-box type composite sections. The upper part of the pylon consists of steel while the lower part beyond the superstructure level is composed of reinforced concrete. The superstructure is located 30m higher than water level. The superstructure is symmetric along the bridge axis while the size of the caisson in PY2 is larger than PY1 due to the difference in water depth. Fig. 3 shows the plan and a cross-sectional view of the bridge.

2.2. FE models

Fig. 4 shows a three-dimensional FE model for the completed structure. The superstructure was modeled with a beam element while stayed cables with an elastic catenary cable element (Kim, *et*

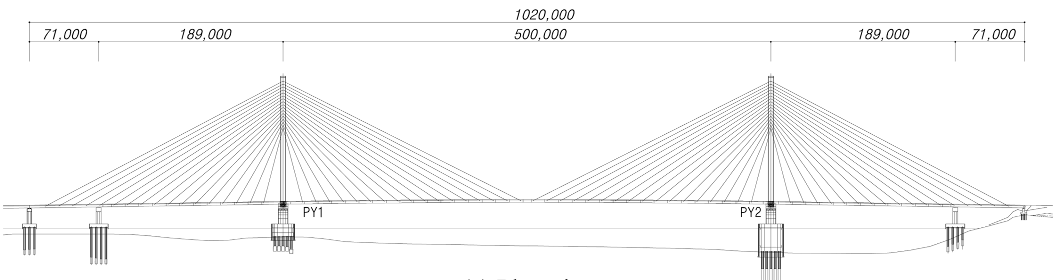

(a) Plan view

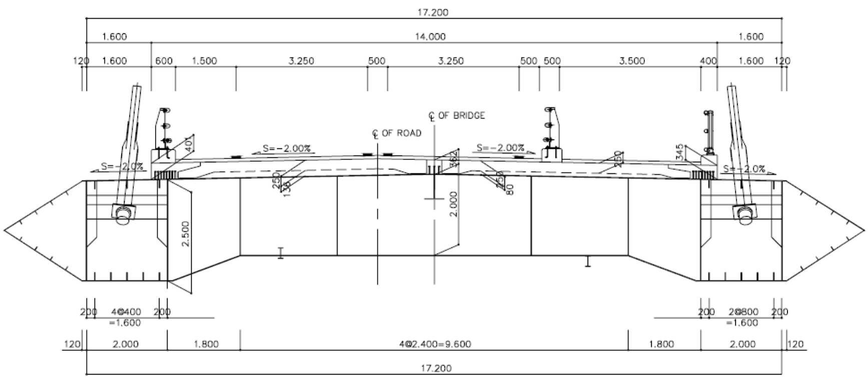

(b) Cross-sectional view of a girder at a cable-anchor position

Fig. 3 The bridge investigated

al. 2006). The pylon was also modeled with a beam element and the caisson and foundation were also included in the model.

Fig. 5 shows the fundamental frequencies and corresponding mode shapes for the completed

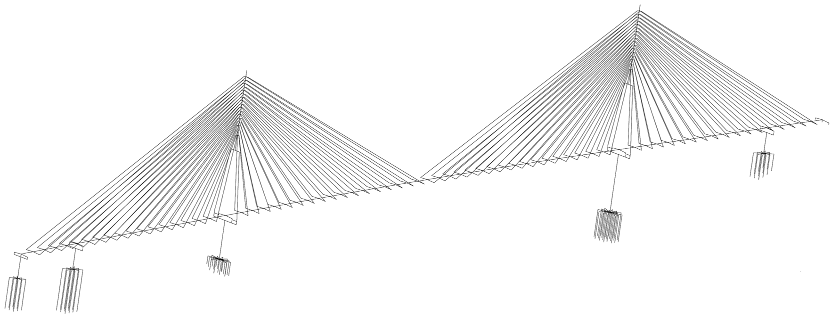

Fig. 4 A three-dimensional FE model

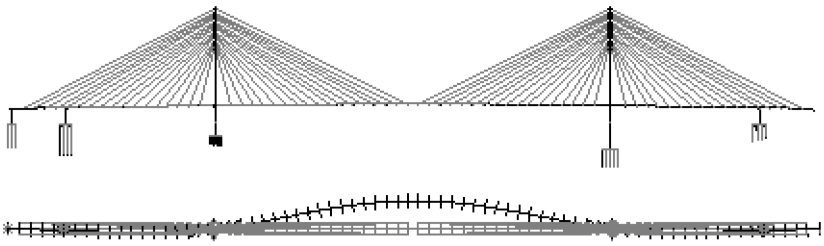

(a) Lateral mode(0.196Hz)

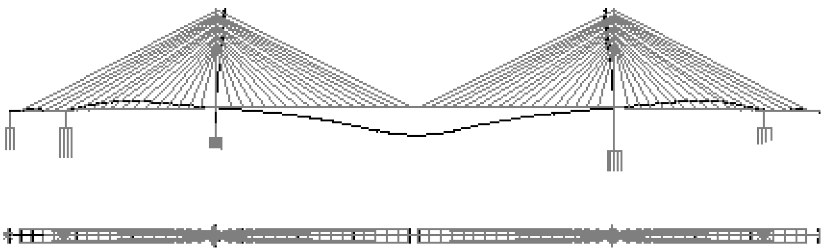

(b) Vertical mode(0.299Hz)

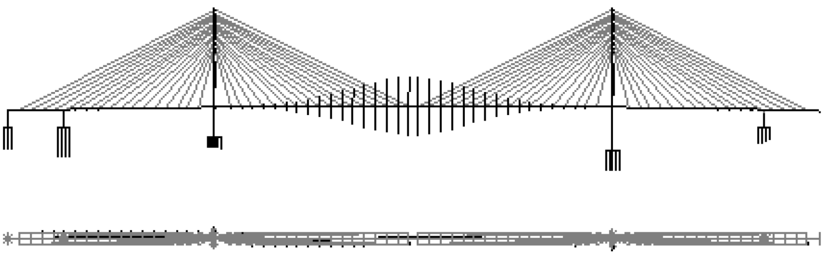

(c) Torsional mode(0.642Hz)

Fig. 5 Fundamental frequencies and mode shapes of the completed structure

structure. Due to the relatively large span-length-to-width ratio (500/17.2 = 29.1), the lateral mode comes out as a first mode of less than 0.2 Hz. The first torsional mode is, however, somewhat higher than other plate-girder cable-stayed bridges, because a two edge-box type cross-section is adopted.

2.3. Buffeting analysis

A single-mode uncoupled buffeting analysis theory (Simiu and Scanlan 1996) was applied in the current study. Since the heaving motion of a bridge deck due to buffeting is a major factor in the design of the stabilizing cables, buffeting loads are only applied to the bridge deck and not to the pylons and stayed cables, which may be rather meaningful in terms of estimating the transverse response in the wind direction. In addition, the seesaw-like motion is dominated by a few lower modes, particularly for the first heaving mode, modal decomposition can be practically applied with the SRSS combination in calculating the total responses.

If $h(x,t)$, $p(x,t)$, and $\alpha(x,t)$ denote the vertical, lateral, and torsional displacement along the bridge deck, respectively, then with the separation of variables into the coordinates x and time t, they can be expressed as the modal summation of the order N.

$$
\begin{aligned}
h(x,t) &= \sum_{i=1}^{N} h_i(x)\xi_i(t) \\
p(x,t) &= \sum_{i=1}^{N} p_i(x)\xi_i(t) \\
\alpha(x,t) &= \sum_{i=1}^{N} \alpha_i(x)\xi_i(t)
\end{aligned}
\tag{1}
$$

The single mode uncoupled equilibrium equation for the mode i can be expressed as follows, with the direct flutter derivatives of H_1^*, P_1^*, A_2^*, and A_3^* for the structure-wind interaction consideration in the form of aerodynamic damping and stiffness (Simiu and Scanlan 1996).

$$
\ddot{\xi}_1 + 2\gamma_i\omega_{i0}\dot{\xi}_i + \omega_{i0}^2\xi_i = \frac{\rho U^2 B}{2I_i}\int_{deck}[Lh_i + Dp_i + BM\alpha_i]dx \tag{2}
$$

where ρ is the density of air, U the mean wind velocity at the deck height, B the deck width, l length of girder, I_i the generalized mass for the i-th mode and

$$
\omega_{i0}^2 = \omega_i^2 - \frac{\rho B^4}{2I_i}\omega^2 A_3^* G_{\alpha_i\alpha_i} \tag{3}
$$

$$
2\gamma_i\omega_{i0} = 2\varsigma_i\omega_i - \frac{\rho B^2}{2I_i}\omega[H_1^* G_{h_ih_i} + P_1^* G_{p_ip_i} + B^2 A_2^* G_{\alpha_i\alpha_i}] \tag{4}
$$

$$
G_{q_iq_i} = \int_{deck} q_i^2(x)dx\,, \quad q_i = h_i,\ p_i,\ \text{or}\ \alpha_i \tag{5}
$$

and

$$L = 2C_L\frac{u}{U} + \left(\frac{dC_L}{d\alpha} + C_D\right)\frac{w}{U} \tag{6}$$

$$D = 2C_D\frac{u}{U} \tag{7}$$

$$M = 2C_M\frac{u}{U} + \frac{dC_M}{d\alpha}\frac{w}{U} \tag{8}$$

where ω_i is the natural frequency of the i-th mode, ω the motional frequency of the deck, ξ_i the damping ratio of the i-th mode, C_L, C_D, and C_M lift, drag, and pitching moment coefficients, $\frac{dC_L}{d\alpha}$ and $\frac{dC_M}{d\alpha}$ the corresponding derivatives, u and w fluctuations in the longitudinal and the vertical wind velocity, respectively.

Using a Fourier transform, the power spectrum for the i-th generalized coordinate can be obtained as

$$S_{\xi_i\xi_i}(\omega) = \frac{\left[\frac{\rho U^2 B}{2I_i\omega_{i0}^2}\right]^2}{\left[1-\left(\frac{\omega}{\omega_{i0}}\right)^2\right]^2 + \left[2\gamma_i\frac{\omega}{\omega_{i0}}\right]^2}\{R_\varphi S_u(\omega) + R_\psi S_w(\omega)\}\frac{1}{U^2} \tag{9}$$

where

$$R_\varphi = \iint_{deck} \varphi(x_A)\varphi(x_B)e^{-C|x_A - x_B|/l}dx_A dx_B \tag{10}$$

$$R_\psi = \iint_{deck} \psi(x_A)\psi(x_B)e^{-C|x_A - x_B|/l}dx_A dx_B \tag{11}$$

where C is the correlation coefficient of the wind velocity fluctuation between two separate points A and B along the bridge deck and

$$\varphi(x) = 2[C_L h_i(x) + C_D p_i(x) + BC_M\alpha_i(x)] \tag{12}$$

$$\psi(x) = \left(\frac{dC_L}{d\alpha} + C_D\right)h_i(x) + B\frac{dC_M}{d\alpha}\alpha_i(x) \tag{13}$$

According to random theory, the variance of ξ_i can be calculated as

$$\sigma_{\xi_i}^2 = \int_0^\infty S_{\xi_i\xi_i}(\omega)d\omega \tag{14}$$

and the SRSS combined root mean square response is

$$\sigma_r = \sqrt{\sum_{i=1}^{N}\phi_i^2\sigma_{\xi_i}^2} \tag{15}$$

where ϕ_i represent the mode shape vector of the i-th mode. $r(t) = \sum_{i=1}^{N}\phi_i\xi_i(t)$, which represents the displacement vector extended to all degrees of freedom for the entire structure in the FE formulation. The maximum response can be obtained by multiplying RMS with the peak factor defined as

$$\bar{K} = (2\ln \nu T)^{1/2} + \frac{0.577}{(2\ln \nu T)^{1/2}} \tag{16}$$

where

$$\nu = \left[\frac{\int_0^{\infty} n^2 S_{\xi_i\xi_i}(n)dn}{\int_0^{\infty} S_{\xi_i\xi_i}(n)dn}\right]^{1/2} \tag{17}$$

and T is the loading duration of the wind velocity fluctuations.

2.4. Member forces

For the design of stabilizing cables, member forces or equivalently corresponding stresses should be calculated and compared with the allowable stress. The modal RMS force, σ_{S_i}, of the frame or cable member i can be calculated by the following random vibration theory.

$$\sigma_{S_i}^2 = [K][T]\{\phi_i\}\{\phi_i\}^T[T]^T[K]^T\sigma_{\xi_i}^2 \tag{18}$$

where, $[K]$ is the element stiffness matrix, $[T]$ the transformation matrix to convert a vector defined in global coordinates to local coordinates, and the superscript T represents the transposition of the matrix.

2.5. Buffeting-related parameters

The design mean wind velocity is assumed 54.9 m/s for the completed structure averaged for 10 minutes at a bridge deck level of 30 m. During construction, this mean wind velocity is reduced to 38.4 m/s, 70% of the completed structure case (Yooshin Engineering Co. 2003).

Static force coefficients of the bridge deck, normalized with the deck width B or B^2, determined through a wind tunnel test as $C_D = 0.183$, $C_L = -0.170$, and $C_M = -0.040$ and the derivatives as $dC_L/d\alpha = -6.106$, and $dC_M/d\alpha = 0.716$ at an attack angle of 0° (Yooshin Engineering Co. 2003). Fig. 6 shows the definition of the force components.

The flutter derivatives are not provided and the current investigation utilized results from other similar bridges as shown in Fig. 7.

A modified Kaimal Spectrum (G.K Fixed Link Co. 2003) was adopted for the longitudinal spectrum S_u and Lumley and Panofsky Spectrum (Simiu and Scanlan 1996) for the vertical spectrum S_w of the fluctuation component in turbulent wind velocity as

$$S_u(z,n) = \frac{144zu_*^2}{U(z)\left(1+36\frac{nz}{U(z)}\right)^{5/3}} \tag{19}$$

$$S_w(z,n) = \frac{3.36zu_*^2}{U(z)\left(1+10\left(\frac{nz}{U(z)}\right)^{5/3}\right)} \tag{20}$$

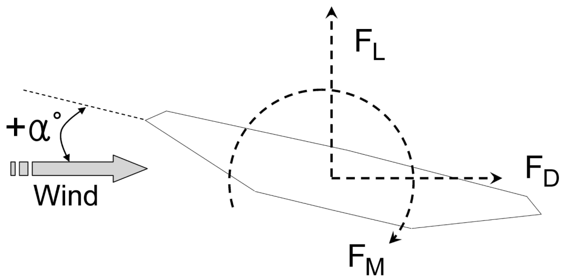

$$C_L = \frac{F_L}{\frac{1}{2}\rho U^2 BL} \quad C_D = \frac{F_D}{\frac{1}{2}\rho U^2 BL} \quad C_M = \frac{F_M}{\frac{1}{2}\rho U^2 B^2 L}$$

Fig. 6 Definition of static force coefficients

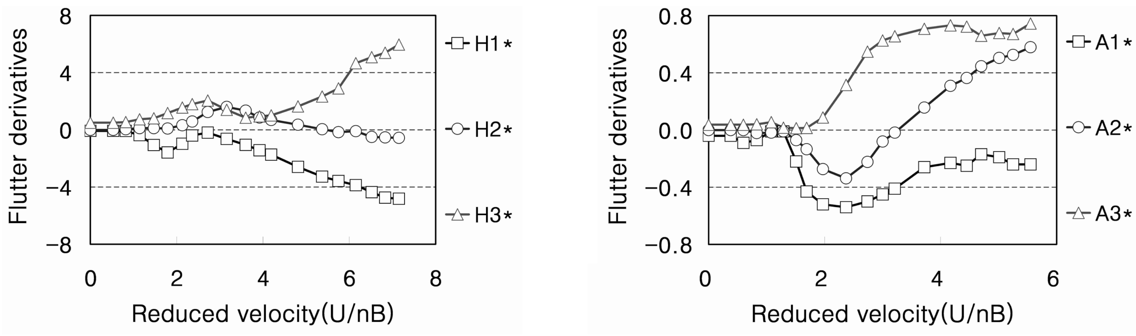

(a) H*

(b) A*

Fig. 7 Flutter derivatives

where n is the frequency(Hz), z the deck level(m), u_* the friction velocity(m/s), $U(z)$ the mean wind velocity at z.

The mean wind velocity at the deck level is calculated by the logarithmic law as

$$U(z) = 2.5u_*\ln(z/z_0) \tag{21}$$

where z_0 is the roughness length (= 0.0075 m). The friction velocity u_* is calculated as follows for the completed structure and the during construction structures, respectively

the completed structure : $u_* = U(30)/2.5\ln(27/0.0075) = 2.648$ m/s
during construction structure : $u_* = U(30)/2.5\ln(27/0.0075) = 1.852$ m/s

Structural damping is assumed 0.5% for all modes and the coefficient C in Eqs. (10) and (11), related to the spatial coherence of wind velocity fluctuations, is assumed to be 8. For safety considerations, aerodynamic admittance is taken as unity for all frequency ranges considered.

2.6. Allowable stress

According to the Design Guideline for Cable-Supported Bridges (KSCE 2005), the load combination related to the wind loads in construction is recommended to consider dead loads, temperatures and wind loads. The recommended increase in allowable stress is 1.5.

The dead load effect was provided by the designer and superposed with the wind effect, which make up the static component due to the mean wind and the dynamic component due to buffeting. Temperature loads were not included in this investigation and as a result, increases in allowable stress were not considered.

For structural safety evaluations, stress is only checked for the steel parts in pylons and box girders in this study. The displacement is also calculated for the girder tip and the top of pylon in a cantilevered structure. Combined stress was evaluated using the following equations proposed by KBDC (KRTA 2005).

$$\text{Stress check : } \left(f_c + \frac{f_{bcy}}{1 - f_c/f_{Ey}} + \frac{f_{bcz}}{1 - f_c/f_{Ez}}\right)/f_{cal} \le 1 \tag{22}$$

$$\text{Stability check : } \frac{f_c}{f_{caz}} + \frac{f_{bcy}}{f_{bagy}(1 - f_c/f_{Ey})} + \frac{f_{bcz}}{f_{bao}(1 - f_c/f_{Ez})} \le 1 \tag{23}$$

where, f_c is the compressive stress due to an axial force, f_{bcy} and f_{bcz} the compressive stresses due to bending moments for the strong(y-axis) and weak(z-axis) axis, respectively, f_{caz} the allowable axial compressive stress, f_{bagy} the allowable bending compressive stress along the strong axis(y-axis) without considering local buckling, f_{bao} the upper limit of allowable bending compressive stress without considering local buckling, f_{cal} allowable local buckling stress for plates, f_{Ey} and f_{Ez} the allowable Euler buckling stresses for the strong(y-axis) and weak(z-axis) axis, respectively.

3. Buffeting responses during construction

3.1. Construction steps considered

Including the final completed structure, three stages of structural systems can be examined to ensure structural safety related to the buffeting-induced vibration. During construction, two critical instances of just before side-span closure and just before center-span closure are considered. Hereafter, these three different status of the structural system are designated as F-N(final completed system, obviously no stabilizing cable), S12-N(just before side span closure on an intermediate pier, no stabilizing cable), and C17-N(just before center span closure, no stabilizing cable). Here, the numbers in the designations represent the number of erected segments of the superstructure on one side of the cantilever from the pylon position. Figs. 8(a) and (b) illustrates the S12-N and C17-N, respectively. The cantilevered structure from PY2 is only considered in further investigations.

During construction, 45^{o}-inclined stabilizing cables are basically installed for securing early stage stability of the first few segments of the superstructure near the pylon, as shown in Fig. 8(c). However, these inclined stabilizing cables have little effect on the structural response when the superstructure is erected to an extent from the pylon. Accordingly, cases S12-N and C17-N actually have inclined stabilizing cables but are regarded as bare structures without mitigation measures in further discussions.

3.2. Natural frequencies and mode shapes

A free vibration analysis is carried out for each investigated case and the natural frequencies for

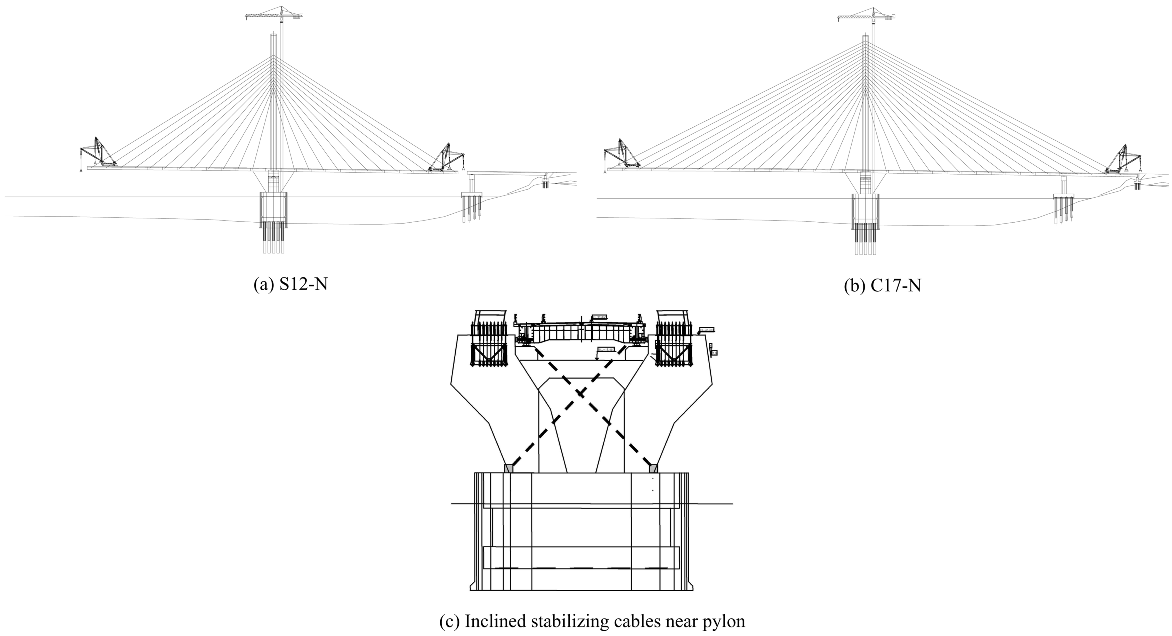

Fig.8 Structures investigated during construction

Table 2 Natural frequencies (Hz) of fundamental modes for each investigated case

Case	Vertical	Lateral	Torsional
F-N	0.299	0.196	0.642
S12-N	0.127	0.316	0.946
C17-N	0.337	0.180	0.729

the fundamental modes are summarized in Table 2.

3.3. Buffeting responses of bare structures

The maximum vertical dynamic displacement reached 2.106m in single amplitude just before side span closure (S12-N) and 0.694m and 0.430m, respectively, for the cases of F-N and C17-N. The maximum lateral dynamic displacement reached 0.304m just before center span closure (C17-N), while the value was 0.297m for the final completed structure (F-N). The maximum torsional dynamic rotation reached 0.012rad for the completed structure. The maximum dynamic displacements are summarized in Table 3.

The combined stresses are calculated for all steel members in a pylon and girder, but only the maximum results are summarized in Table 4 for each investigated case. According to Table 4, the steel members in a pylon at the stage of S12-N exceed the allowable limit by a considerable extent, showing the necessity of stabilizing cables or other measures during the construction process.

Steel members in a girder at the completed stage are also expected to exceed allowable limit by 20%. For this investigation, only the dead load and wind load are considered, as previously mentioned. If temperature is also included in the load combination, the allowable stress increases by

Table 3 Maximum dynamic displacements of the deck in a single amplitude for each investigated case

Case	Vertical(m)	Lateral(m)	Torsional(rad)
F-N	0.694	0.297	0.0120
S12-N	2.106	0.077	0.0025
C17-N	0.430	0.304	0.0071

Table 4 Maximum stress in pylon and girder for each investigated case

Case	Stress check for pylon	Stability check for pylon	Stress check for girder	Stability check for girder
F-N	0.81	0.85	1.18	1.21
S12-N	1.45	2.46	0.58	0.61
C17-N	0.66	0.70	0.66	0.69

50%, which would be expected to be much higher than the stress increase due to a temperature load in the engineering sense. A more detailed check can be followed in the final design stage, but any other measure is not considered to be a completed structure at this moment.

3.4. Stabilizing measures

Stabilizing measures are, therefore, only investigated for the just before side-span closure stage (Case S12-N). Available measures have already been discussed in Fig. 2 and the vertical stabilizing cables are the main focus of the current investigation.

4. Design of stabilizing cables

4.1. Generals

The installing positions, the number of strands and the pretension of stabilizing cables were determined in the preliminary design process. The positions of the stabilizing cables were determined only considering the mitigation effect on dynamic buffeting responses because the mean wind static response is relatively small compared to the dynamic one due to the small lift coefficient. A stress check and other design processes were, however, carried out considering dead loads, mean wind static load, buffeting load and cable tensions due to the pretension of stabilizing cables, if any.

4.2. Reviewed structures regarding installation of the stabilizing cables

Fig. 9 shows the arrangement of the stayed cables with other structural supports for girders such as the internal pier, the end pier and the pylon. By considering the distance between the pylon and the internal pier, one set of vertical stabilizing cable is examined for installation between stayed cables No. 5 and No. 8. Since the navigation channel is secured in another route during the construction, the plan is to install the stabilizing cable symmetrically on both sides of the cantilevered spans as shown in Fig. 2(b).

The critical stages to be reviewed for dynamic safety can be determined considering the following check points.

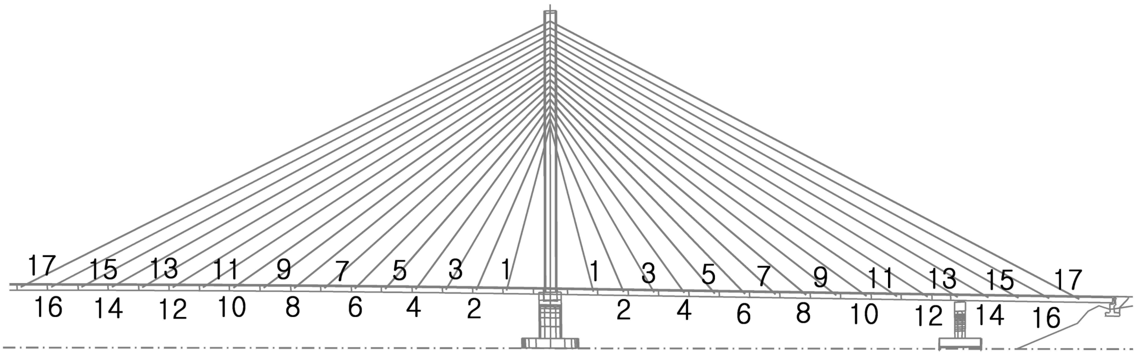

Fig.9 Arrangement of stayed cables

Check point 1: Is the structure safe just before the installation of the stabilizing cables?
Check point 2: Is the structure safe just before the side span closure on the internal pier with stabilizing cables?

For better performance for check point 1, the position of the stabilizing cable should be shifted to No. 5, while it leads worse performance for the check point 2, and vice versa. For this reason, an optimal position should be determined so as to balance both check points by altering the position of the stabilizing cables from the position of stayed cable No. 5 to No. 8.

In relation to check point 1, is there any possibility of utilizing the temporary anchorages prepared for the vertical stabilizing cables even when the structure is not sufficiently erected to the position of the vertical stabilizing cable installation? In this case, more weight can be shifted to check point 2 than check point 1 to increase the safety for the most critical stage just before side-span closure. This may be possible by connecting the stabilizing cables with some inclination from the cantilever tips to the temporary anchors prepared for the installation of the vertical stabilizing cables (refer to Fig. 11(b)). In relation with this, the following check point is added.

Check point 3: When stabilizing cables are installed from the cantilever tips to the temporary anchors prepared for the installation of the vertical stabilizing cables with some inclinations, how much stabilizing effect can be expected? Is this preparation worthwhile?

Taking all of the check points 1, 2, and 3 into consideration, 15 structural cases that require comparative examinations are determined and the results are summarized in Table 5.

4.3. Natural frequencies

Table 6 shows the variation in fundamental natural frequencies for each of the cases reviewed. As the cantilevered length increases from S5-N to S12-N, the lowest vertical, lateral and torsional modes gradually decrease and, as a result, the buffeting responses are expected to increase.

By comparing the first lateral frequencies for the cases of S12-V5~S12-V8 with S12-N, it would be expected that the lateral response would not be influenced by the installation of a vertical stabilizing cable. When the vertical stabilizing cables were installed further away from the pylon,

Table 5 Structural cases reviewed for determining the position of the stabilizing cable

Check points*)	Case	Reviewed structural system**)	Anchor position of stabilizing cable on girder	Position of dead anchor block in seabed
Check point 1	S5-N	Step 5	N (no stabilizing cable)	N (no stabilizing cable)
	S6-N	Step 6		
	S7-N	Step 7		
	S8-N	Step 8		
	S12-N	Step 12		
Check point 2	S12-V5	Step 12	V5 (vertical stabilizing cable on No.5)	V5 (No.5)
	S12-V6		V6 (vertical stabilizing cable on No.6)	V6 (No.6)
	S12-V7		V7 (vertical stabilizing cable on No.7)	V7 (No.7)
	S12-V8		V8 (vertical stabilizing cable on No.8)	V8 (No.8)
Check point 3	S5-T6	Step 5	S5 (inclined stabilizing cable on No.5)	T6 (No.6)
	S5-T7	Step 5	S5 (inclined stabilizing cable on No.5)	T7 (No.7)
	S6-T7	Step 6	S6 (inclined stabilizing cable on No.6)	T7 (No.7)
	S5-T8	Step 5	S5 (inclined stabilizing cable on No.5)	T8 (No.8)
	S6-T8	Step 6	S6 (inclined stabilizing cable on No.6)	T8 (No.8)
	S7-T8	Step 7	S7 (inclined stabilizing cable on No.7)	T8 (No.8)

*) The definition of check points are illustrated in Section 4.2.
**) e.g. Step 5 denotes that the cantilevered superstructure is currently erected to the position of the stayed cable No. 5. (See Fig. 9 for the stayed cable number.)

i.e. S12-V8, the natural frequency for the first vertical mode, as expected, increased due to the stabilizing effect of the larger moment arms of the vertical cables.

4.4. The positions of installation of the stabilizing cables

The position of installation of the vertical stabilizing cables should be determined with the stabilizing effect and construction cost taken into consideration. The stabilizing effect can be estimated from the buffeting responses of the displacements (*e.g.*, the vertical displacement of the cantilever tips and/or the horizontal displacement of the pylon top) or sectional forces (*e.g.*, bending moments at several check points in the pylon and girders). Construction costs may be estimated from the maximum tensions of the vertical stabilizing cables, which are directly related to the size of the concrete blocks that hold down the cable in the seabed.

The check points for buffeting-induced member forces or equivalent stresses in a pylon are shown

Table 6 Fundamental natural frequencies (Hz) for the reviewed structural cases during construction

Case	1st vertical	1st lateral	1st torsional
S5-N	0.294	1.370	1.556
S6-N	0.265	1.031	1.432
S7-N	0.236	0.803	1.313
S8-N	0.208	0.642	1.231
S12-N	0.127	0.316	0.964
S12-V5	0.294	0.316	0.971
S12-V6	0.346	0.316	0.995
S12-V7	0.408	0.317	1.039
S12-V8	0.485	0.317	1.114
S5-T6	0.552	1.368	1.904
S5-T7	0.558	1.368	1.835
S6-T7	0.566	1.030	1.730
S5-T8	0.517	1.368	1.716
S6-T8	0.573	1.030	1.652
S7-T8	0.561	0.802	1.575

in Fig. 10. Section A-A represents the transition point for the separation to two legs, section B-B the connection point between the steel pylon and the concrete pier, and section C-C the bottom of the caisson.

The buffeting responses are presented in Table 7 for each of the cases reviewed. The buffeting responses for the critical stage (S12-N, i.e., just before side-span closure without a stabilizing cable) exceed the allowable limit, as described in section 3.3.

Before the vertical stabilizing cables are installed, the cantilever structure should be resisted by the bare structure itself. Accordingly, if it is assumed that the vertical cable is installed at the position No.7 in terms of the stayed cable number on the stiffening girder, the longest free cantilever structure before the vertical cable installation (S6-N) should be also safe with respect to buffeting excitations. As shown in Table 7, all of the buffeting responses increase with increasing free cantilever length from S5-N to S8-N. As a result, if check point 1 mentioned in Section 4.2 is the only concern, it may be preferable to install the vertical stabilizing cable as close to the pylon as possible.

Moving to check point 2, which is related to the most critical stage, i.e., just before side span closure. From 6th to 9th rows in Table 7 represent the buffeting responses at this critical stage with vertical stabilizing cables installed at positions No.5, No.6, No.7, or No.8 in terms of the stayed cable number (represented as S12-V5, S12-V6, S12-V7, and S12-V8, respectively). All of the cases produced more stable behavior than the bare structure without stabilizing cables, i.e., S12-N. As the vertical cables were installed closer to the pylon, *e.g.* S12-V5, the maximum tensions of the vertical stabilizing cables tended to increase, and therefore, larger sized dead anchor blocks were required in the seabed. The displacement at the cantilever tip also increased, and as a result, overall behaviors were less competitive except for the bending moment at the caisson bottom. Accordingly, if check point 2 is only of concern, it may be preferable to install the vertical stabilizing cable as far from the pylon as possible.

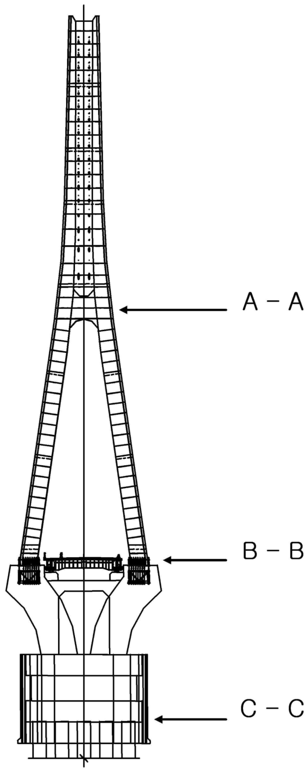

Fig. 10 Check points for maximum stresses in pylon

The check points 1 and 2 conflict with each other, and the final position of the vertical stabilizing cable may be No. 7 in terms of stayed cable number, as shown in Fig. 11(a). Note that, even for this case, the buffeting responses before the installation of the vertical cables (S5-N and S6-N) exceeded the responses just before side span closure (S12-V7), as shown in Table 7. If the maximum stresses are limited to the allowable range, it should be fine as it is.

Other measures, however, can also be considered, such as the use of designed dead anchors in the seabed. One of these is the installation of stabilizing cables even though the stiffening girder is not installed up to the position of 7, *e.g.*, S6-T7 as shown in Fig. 11(b). According to Table 7, this measure appears to be very effective for controlling buffeting response, similar to the vertical stabilizing cables. However, extra anchoring devices on the stiffening girder segments located at position No.5 and/or No.6 are required.

Based on the above discussions, this study proposes that the vertical stabilizing cable could be installed at No.7 in terms of the number of stayed cable anchorages on the stiffening girder.

4.5. Required number and pretension of stabilizing cables

The maximum tensions of the stabilizing cables were also estimated by means of a buffeting analysis. The downward deflection of the stiffening girder can possibly lead to the stabilizing cable becoming slack. This may result in the cable socket pulling out from the anchorage, unless special devices are provided. Furthermore, since slacking denotes a loss of stiffness of the vertical stabilizing cables, it can not be considered in the current frequency domain linear buffeting analysis.

Table 7 Maximum buffeting responses in a single amplitude for each reviewed case

Case	Tension of Stabilizing cable (kN)	Displacement (m)		Along-bridge-axis bending moment (kNm)		
		Vertical at the tip of cantile-vered girder	Horizontal at the Top of pylon	Section A-A	Section B-B	Section C-C
S5-N		0.28	0.54	70,800	54,170	344,550
S6-N		0.41	0.67	87,720	66,370	385,360
S7-N		0.58	0.80	105,840	80,730	418,430
S8-N		0.79	0.94	125,230	97,560	451,400
S12-N		2.11	1.66	211,430	187,730	616,010
S12-V5	1,501	0.47	0.31	21,470	53,430	171,550
S12-V6	1,315	0.37	0.23	15,350	39,680	181,630
S12-V7	1,207	0.31	0.17	14,300	29,640	225,150
S12-V8	1,128	0.25	0.13	17,110	23,060	372,940
S5-T6	373	0.02	0.10	12,130	16,780	206,010
S5-T7	432	0.03	0.12	14,690	18,680	230,290
S6-T7	481	0.04	0.11	15,740	19,130	247,280
S5-T8	628	0.05	0.20	23,900	24,670	179,340
S6-T8	559	0.05	0.13	19,130	20,070	321,180
S7-T8	579	0.06	0.12	20,840	18,150	339,630

Slacking can be avoided by pre-tensioning stabilizing cable with an amount at least equal to the maximum expected compressive axial force, or, equivalently the maximum expected loss of tension, in the stabilizing cable due to the single amplitude of the buffeting responses. In this case, the maximum tensions of the stabilizing cables reach twice the single amplitude maximum buffeting tension when pretension is considered.

Table 8 shows the installing pretension and the expected maximum tension for each structural case. The maximum tension of the inclined cables near the pylon are expected at stage S6-N(bare structure before vertical cable installation) and reached 1,756 kN, while the vertical cables at stage S12-V7(before the side span closure) reached 2,404 kN.

A 7-wire strand (7-5.1Φ) is used for the stabilizing cables and the cross-sectional area of one strand is 0.00015 m^2. The allowable stress is taken to be 0.45 f_S, and the allowable tension of one strand is 118.7 kN. The required number of strands was calculated to be 15 and 20 for the inclined and the vertical stabilizing cables, respectively. This study proposes the following dimensions for the stabilizing cables.

- Inclined cable: 20-strand (0.003 m^2) each, and total 8EA for both cantilevered structures at PY1 and PY2
- Vertical cable: 25-strand (0.00375 m^2) each, and total 8EA for both cantilevered structures at PY1 and PY2

4.6. Required weight of the dead anchor blocks

The maximum tension of each of the vertical stabilizing cable is 2,404 kN. Since two vertical

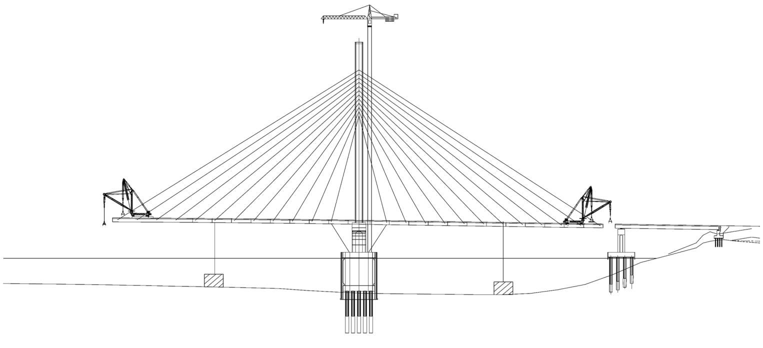

(a) S12-V7

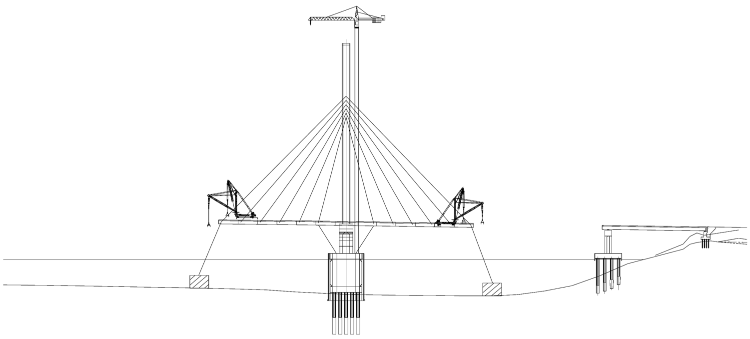

(b) S6-T7

Fig. 11 Selected stabilizing strategies

Table 8 Calculation of the required pretension and the dimensions of the stabilizing cables

Case	Required pretension (kN)				Maximum tension (kN)			
	Inclined cables		Vertical cables		Inclined cables		Vertical cables	
	Center span	Side span	Center span	Side span	Center span	Side span	Center span	Side span
S6-N	853	873	-	-	1,706	1,756	-	-
S12-V5	245	245	1,491	1,501	490	490	2,972	3,012
S12-V6	235	235	1,295	1,315	470	470	2,590	2,630
S12-V7	235	235	1,187	1,207	470	470	2,374	2,404
S12-V8	235	245	1,109	1,128	470	490	2,218	2,256
C17-N	275	275	-	-	550	550	-	-
Expected maximum					1,706	1,756	2,374	2,404
Calculated number of strands					15	15	20	20
Proposed number of strands					20	20	25	25

cables are installed at both sides of the cross-section of the stiffening girder, the required counterweight should be larger than 4,808 kN. If concrete dead blocks are used for anchorages, the total weight of the blocks should be determined by considering the buoyancy.

4.7. Summary of the stabilizing effect

According to the determined position of the vertical stabilizing cable, the following critical structural stages were selected and investigated.

- S6-N : bare structure just before the installation of vertical stabilizing cables (Check Point 1)
- S12-V7 : just before the side span closure with vertical stabilizing cables at position No.7 (Check Point 2)
- S6-T7 : temporal inclined stabilizing cables between the girder position of No. 6 with a dead anchor located at position No.7 in the seabed (Check Point 3)

The bare structure case at the critical stage of just before the side span closure (S12-N) is also provided for the stabilizing effect comparison.

Table 9 shows the maximum displacement of the stiffening girder. Without stabilizing cables, the vertical displacement just before side span closure (S12-N) reached 2.226 m. By applying vertical stabilizing cables (S12-V7), this displacement decreased to 0.320m. Prior to the installation of the vertical cables (S6-N), the cantilever tip displacement reached 0.416m, which exceeds the vertical displacement at the most critical stage of side span closure with stabilizing cables (S12-V7). This vibration can also be reduced to 0.041 m by applying stabilizing cables between the cantilever tips to existing dead blocks with inclination (S6-T7).

According to the Table 9, the proposed stabilizing cables are only effective in mitigating the vertical responses of the stiffening girder. To mitigate lateral or torsional responses, other types of stabilizing measures may be used if required. In this investigation, however, stress calculations were done by combining the axial force and two perpendicular bending moments including lateral vibration effect and there was no need to control lateral motion of the cantilevers.

Table 10 shows the gust factors for the displacement of a stiffening girder. The gust factor is defined as the response ratio of the mean wind plus buffeting to the mean wind. As shown in Table 10, the lateral response can be predicted by multiplying the mean wind response by the gust factor (e.g. 1.7~1.9). However, the vertical response can not be predicted in the same way and this illustrates the necessity of using a buffeting analysis in the design of stabilizing cables.

Table 9 Maximum displacements for a stiffening girder for the constructional stages reviewed

Case	Vertical (m)			Lateral (m)			Torsional (rad)		
	Buffeting	Mean wind	Total	Buffeting	Mean wind	Total	Buffeting	Mean wind	Total
S6-N	0.412	0.004	0.416	0.006	0.015	0.021	0.0013	0.0001	0.0014
S12-N	2.106	0.120	2.226	0.078	0.089	0.166	0.0025	0.0002	0.0027
S12-V7	0.308	0.012	0.320	0.078	0.089	0.167	0.0022	0.0005	0.0027
S6-T7	0.039	0.002	0.041	0.005	0.015	0.020	0.0010	0.0001	0.0011

Table 10 Gust factors for the displacement of a stiffening girder at the tip of the cantilever

Case	Vertical	Lateral	Torsional
S6-N	0.416/0.004 = 104	0.021/0.015 = 1.4	0.0014/0.0001 = 14
S12-N	2.226/0.120 = 19	0.166/0.089 = 1.9	0.0027/0.0002 = 14
S12-V7	0.320/0.012 = 27	0.167/0.089 = 1.9	0.0027/0.0005 = 5
S6-T7	0.041/0.002 = 156	0.020/0.015 = 1.3	0.0011/0.0001 = 11

Table 11 Stress check for the combined loads

Case	Pylon		Stiffening girder	
	Stress (Eq. 22)	Stability (Eq. 23)	Stress (Eq. 22)	Stability (Eq. 23)
S6-N	0.64	0.83	0.36	0.38
S12-N	1.45	2.46	0.58	0.61
S12-V7	0.56	0.61	0.53	0.57
S6-T7	0.36	0.34	0.31	0.35

The stress checks in Eqs. (22) and (23) were carried out for the combined loads of dead loads, mean wind loads, buffeting loads, and pretensions due to the installation of a stabilizing cable. The results are summarized in Table 11. By applying a vertical stabilizing cable, the stresses at the critical stage of the side span closure (S12-V7) are within the allowable range. Prior to the installation of a vertical stabilizing cable, the stresses are also within the allowable range. However, for the purpose of safety considerations, the earlier use of stabilizing cable with inclination (S6-T7) provided a more stable performance.

5. Conclusions

A design procedure for the installation of stabilizing cable is proposed for the construction of a cable-stayed bridge by the use of a buffeting analysis. Since the buffeting-induced stresses exceeded the allowable range for a free cantilevered structure, a set of stabilizing cables is planned to mitigate seesaw-like motion. The design procedure includes judging the necessity of a stabilizing cable, the determination of installing positions, the number of strands needed, the required pretension of the stabilizing cable and the corresponding dead weight to hold the cables down.

According to the proposed measurement with vertical stabilizing cables, the free cantilevered structure would be expected to secure aerodynamic safety for upcoming turbulence during the construction process.

The numerical results are based on some assumptions due to unavailable parameters at the design stage and hopefully will be updated in the future if wind-tunnel tests can provide additional aerodynamic and aeroelastic parameters related to a more reliable buffeting analysis.

Acknowledgement

This research was supported by a grant(05RCB05-01) from regionally characterized construction technology program funded by Ministry of Construction & Transportation of Korean Government.

References

Chauvin, A., Revelo, C. K., Raggett, J. D. and Scanlan, R. H. (1994), "Mezcala bridge-Mexico; Wind effects modelling and structural analysis", *Proceedings of the international Conference on Cable-stayed and Suspension Bridges*, (2), 127-134.

Conti, E., Grillaud, G., Jacob, J. and Cohen, N. (1994), "Wind effects on the Normandie cable-stayed bridge: Comparison between full aeroelastic model tests and quasi-steady analytical approach", *Proceedings of the International Conference on Cable-stayed and Suspension Bridges*, (2), 81-90.

G.K Fixed Link Co. (2003), *Design Criteria of the Busan-Geoje Fixed Link Project*.

Kim, H. K., Lee, M. J. and Chang, S. P. (2006), "Determination of hanger installation procedure for a self-anchored suspension bridge", *Eng. Struct.* **28**, 959-976.

Kimura, K., Nakamura, S. and Tanaka, H. (1994), "Buffeting analysis for cable-stayed bridges during construction in yawed wind", *Proceedings of the international conference on cable-stayed and suspension bridges*, (2), 109-16.

KRTA(Korea Road & Transportation Association). (2005), *Korean Bridge Design Code(KBDC)*.

KSCE(Korean Society of Civil Engineers). (2005), *Design Guidelines for Cable-supported Steel Bridges*.

Larose, A. and Livesey, F.M. (1994), "On cable-stayed bridges during construction: Modeling and prediction of aerodynamic behavior", *Proceedings of the International Conference on Cable-stayed and Suspension Bridges*, (2), 73-80.

Shum, K. M., Xu, Y. L. and Guo, W. H. (2006), "Buffeting response control of a long span cable-stayed bridge during construction using semi-active tuned liquid column dampers", *Wind Struct.*, *An Int. J.* **9**(4), 271-296.

Simiu, E. and Scanlan, R. H. (1996), *Wind Effects on Structures,* John Wiley & Sons.

Tanaka, H., Larose, G. L. and Kimura, K. (1998), "Aerodynamics of long-span bridges during erection", *Proceedings of the Advances in Bridge Aerodynamics International Symposium*, 119-127.

Virlogeux, M. (1992), "Wind design and analysis for the Normandy Bridge", *Proceedings of the Aerodynamics of large bridges 1st International symposium*, 183-216.

Yooshin Engineering Co. (2003), *Report of wind-tunnel test and CFD analysis for the Dolsan-Hwatae Bridge*.

CC